Available online at www.sciencedirect.com
ScienceDirect
Current Opinion in Structural Biology

Unveiling invisible protein states with NMR spectroscopy

T Reid Alderson[1,2,3] and Lewis E Kay[1,2,3,4]

Proteins interconvert between multiple conformations, including sparsely populated and transiently formed states that are difficult to characterize in structural detail using standard biophysical methods. In some cases, changes to the dynamical equilibria between conformations can lead to pathological protein aggregation and to the disruption of cellular homeostasis. The detection and characterization of lowly populated conformers is therefore crucial for understanding the basis of protein misfolding. NMR spectroscopy is exquisitely sensitive to the conformational dynamics of biomolecules and can be used to study sparsely populated states at the atomic level. Here, we review recent progress toward understanding the roles of sparsely populated, otherwise 'invisible' states present in protein folding and misfolding, where NMR has provided unique insight into folding intermediates, transiently misfolded states, and soluble oligomers that precede amyloid fibril formation.

Addresses
[1] Department of Biochemistry, The University of Toronto, ON, M5S 1A8, Canada
[2] Department of Molecular Genetics, The University of Toronto, ON, M5S 1A8, Canada
[3] Department of Chemistry, The University of Toronto, ON, M5S A18, Canada
[4] Program in Molecular Medicine, The Hospital for Sick Children, Toronto, ON, M5G 1X8, Canada

Corresponding authors: Alderson, T Reid (reid.alderson@utoronto.ca), Kay, Lewis E (kay@pound.med.utoronto.ca)

Current Opinion in Structural Biology 2020, **60**:39–49

This review comes from a themed issue on **Folding and binding**

Edited by **Shachi Gosavi** and **Benjamin Schuler**

For a complete overview see the Issue and the Editorial

Available online 11th December 2019

https://doi.org/10.1016/j.sbi.2019.10.008

Introduction

Proteins are not static molecules but populate a range of structural states that dynamically interconvert on a multitude of timescales [1,2]. These motions range from local backbone fluctuations and aromatic ring flips to inter-domain structural rearrangements and the exchange of oligomeric subunits. Many important cellular signaling pathways depend on the dynamical nature of proteins that enables their reversible transition between different structural forms [3–5]. As such, the dysregulation of protein dynamics can severely impact human health: disease-causing mutations that do not perturb the fold of a protein can drastically shift its dynamical equilibrium toward otherwise sparsely populated conformations [6••] with enhanced aggregation or degradation propensities [7] or dysregulated interactions with other biomolecules [8–10] or pharmaceuticals [11]. More generally, rare conformers impact the fidelity of the central dogma: DNA polymerases misincorporate G·T base pairs because of lowly populated nucleotide tautomers [12••].

Characterizing the dynamical equilibria of functionally relevant protein states has remained challenging, however, since the lowest energy or most abundant conformer is the one typically captured by methods such as X-ray crystallography or cryo-electron microscopy (cryo-EM). Understanding the functions and dysfunctions of proteins in health and disease, however, requires a quantitative characterization of the thermally accessible conformational landscape, including a description of the dynamics, structures, and relative populations of the conformers that populate it [6••]. Over the past decade, significant progress has been made toward the understanding of sparsely populated protein states and their functional roles in a variety of biological processes [13,14]. Here, we highlight the role of NMR spectroscopy in providing structural and dynamical insight into otherwise invisible, low-populated protein conformations [15] that are present during protein folding and misfolding (Figure 1). Such conformations can expose hydrophobic regions or make transient inter-molecular interactions that can initiate the pathogenic process of aggregation (Figure 1). We discuss insights from NMR-based chemical exchange and rapid pressure-jump experiments that have provided the ability to structurally characterize sparsely populated, otherwise invisible conformations with unprecedented, atomic-level detail [16•].

Folding

The folding of proteins from unstructured polypeptide chains into exquisite three-dimensional structures plays a pivotal role in human health [17]. Seemingly disparate diseases such as type II diabetes, cystic fibrosis, amyotrophic lateral sclerosis, chronic traumatic encephalopathy, and Alzheimer's share a common molecular origin: the misfolding of proteins [17]. Inside the crowded environment of the cell, misfolded proteins that expose hydrophobic regions can readily self-associate into

Figure 1

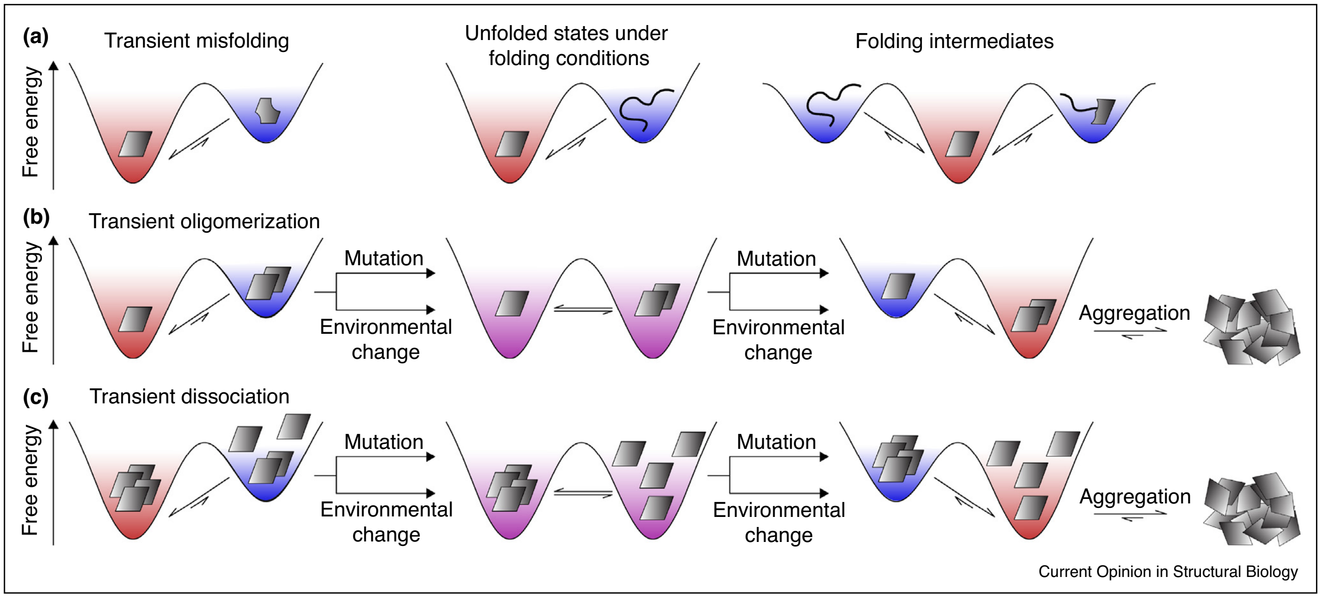

NMR can probe a wide range of sparsely populated protein conformers. For a protein present in conditions that favor its folded state, higher-energy states in exchange with the ground state might entail **(a)** (left) a locally misfolded conformer, (middle) the unfolded chain, or (right) a folding intermediate. In the latter case, three-state exchange is depicted to reflect interconversion between the ground state and the unfolded chain as well as the ground state and a partially structured intermediate. Other kinetic models are of course possible. **(b)** An aggregation-prone protein can transiently sample a higher-energy, non-native dimer or other oligomeric state. **(c)** Likewise, a native oligomer can dissociate into its constituent subunits and monomers. Mutations or other environmental changes — such as alterations to the pH, temperature, pressure, or concentration of salt, denaturant, or protein — could shift the free energy difference between states, eventually inverting the populations. In some cases, non-native oligomers or free monomers can be highly prone to aggregation. Sparsely populated states can also occur in other biological processes, including enzyme catalysis and molecular recognition, which are not discussed here.

cytotoxic aggregates. Cellular homeostasis therefore requires the maintenance of favorable conditions for protein folding, as well as dedicated machinery to actively counteract misfolding and aggregation. In order to fold properly, some proteins require the assistance of molecular chaperones, such as heat shock protein 70 and 90 (Hsp70 and Hsp90); however, the amino acid sequences of many proteins encode the ability to correctly and autonomously fold to their native conformations within microseconds to milliseconds.

A major goal of *in vitro* biophysical studies of protein folding has long been to elucidate the molecular details that determine how proteins fold into their final structures, as well as the conformations of metastable intermediate states that are populated along the folding pathway. Historically, folding studies have taken place *in vitro* by rapid mixing or a sudden change in conditions, with typical mixing agents including chemical denaturants, salts, acids, or bases and changes in conditions including jumps in temperature or pressure. Arguably the most benign denaturing agent, hydrostatic pressure has been used for decades to study protein folding [18], as it can shift the relative populations in the free energy landscape of a protein under otherwise native buffer conditions, provided that a volumetric difference exists between the respective states [19,20].

New folding insights from pressure-jump NMR

Protein folding-by-NMR studies using pressure were previously limited by the long time required for pressure changes and equilibration [18]; however, new hardware developments have enabled rapid switching of the pressure inside the NMR sample in the span of a few milliseconds. These advances have opened a new avenue for the study of protein folding at the atomistic level with millisecond time resolution [21,22••,23,24]. It has thus become possible to measure hydrogen exchange rates [21] and chemical shifts [22••,23,24] during folding, with nuclear Overhauser effects (NOEs) and residual dipolar couplings (RDCs) likely also feasible.

Charlier *et al.* studied a variant of ubiquitin, which included two Val to Ala substitutions (VA2-ubiquitin) that were necessary to unfold the protein at experimentally accessible pressures (<3 kbar). The ability to rapidly jump the pressure from denaturing to native conditions and record high-resolution NMR spectra during folding led to the identification of parallel folding pathways, $U \xrightarrow{k_{UI}} I \xrightarrow{k_{IF}} F$ and $U \xrightarrow{k_{UF}} F$, the former including a transient, on-pathway intermediate, I [22••]. A stroboscopic approach to effectively 'snapshot' the ensemble-averaged chemical shifts as a function of folding time provided structural insight into the folding intermediate: ^{15}N and ^{13}CO chemical shifts indicated that it had comparable structure to the native state, except for deviations in its first and last β-strands, as well as the loop preceding the final strand [23,24]. These initial pressure-jump NMR studies have yielded novel insight into the folding pathway of ubiquitin, and the approach holds significant promise of providing an atomistic view into the folding mechanisms of pressure-sensitive proteins or their pressure-sensitized variants.

Residual structure in the unfolded states of folded proteins

While the above studies sought to characterize structured intermediates, significant effort has also focused on the unfolded states of proteins under native conditions. Does native-like structure persist in the unfolded chain? Using rapid pressure-jump technology to reversibly unfold VA2-ubiquitin, Charlier *et al.* structurally characterized the unfolded state under folding conditions before its crossing the transition-state barrier. They found that the not-yet folded protein transiently forms its N-terminal β-hairpin [21,22••], as well as a non-native α-helix near the center of the protein [22••].

Using Carr-Purcell-Meiboom-Gill (CPMG) relaxation dispersion (RD) NMR (Box 1) under native conditions, Pustovalova *et al.* characterized the structural propensities of the unfolded state of the activation domain of procarboxypeptidase A2 (ADA2h), which adopts a mixed α/β fold in its native state but can readily form β-strand-rich amyloid fibrils. The natively unfolded state was populated to ca. 1% at room temperature (Box 1), and relaxation dispersion experiments demonstrated that residual native-like structure persists in regions corresponding to helices in the folded state whereas the sites that form strands were disordered and flexible [25]. Chemical shifts and RDCs measured from the sparsely populated unfolded state were subsequently used as restraints in molecular dynamics simulations to characterize its conformational landscape [26]. It is interesting to note that the otherwise unrelated protein gpW, which folds into a mixed α/β fold within microseconds, also contains residual helicity in its natively unfolded state whereas its β-hairpin had fully unfolded [27,28].

Chaperone-substrate interactions

Finally, NMR spectroscopy has proved indispensable in characterizing the dynamic nature of proteases [29], molecular chaperones [30,31] and the conformations of their transiently bound substrates [32•,33–35]. The unique ability of NMR spectroscopy to monitor transient, weak interactions has shed light on the activity of Hsp70 and other molecular chaperones, including substrate binding to the AAA + ATPase VAT [36,37]. Some of these topics have been reviewed elsewhere [30,33], and thus we will focus our discussion here only on substrate binding to Hsp70 [38,39,40•]. The Hsp70 substrate human telomere repeat factor 1 (hTRF1), which folds into a three-helix bundle, populates a natively unfolded conformation to ca. 4% with a lifetime of ca. 3 ms in solution at 25 °C. Backbone chemical shifts measured for the natively unfolded conformation obtained with ^{15}N, ^{13}Cα, and ^{13}Cβ chemical exchange saturation transfer (CEST) [41] (Box 1) were indicative of a disordered protein with partially helical secondary structure. Interestingly, binding of the bacterial Hsp70 chaperone DnaK to hTRF1 promoted global unfolding and adoption of the same secondary structural preferences as in the natively unfolded form, indicating that Hsp70 does not remodel the inherent secondary structural propensities of the unfolded chain [39]. Moreover, Sekhar *et al.* found that DnaK binding abolished the transient long-range tertiary contacts that were otherwise present in the natively unfolded form of hTRF1 [38].

But how does Hsp70 bind to substrates: does it first bind to the structured form and, via induced fit, remodel the substrate to its unfolded conformation? Or does Hsp70 use a conformational selection mechanism whereby it selectively binds to the natively unfolded state that is present at equilibrium? Through a combination of magnetization-exchange [42] and CEST-based relaxation measurements, both the bacterial and human forms of Hsp70 were found to bind to two different substrates via conformational selection [40•]. The Hsp70 chaperone therefore selectively binds to the unfolded conformation of substrates [40•] and prevents the formation of tertiary contacts but enables the bound polypeptide chain to sample its inherent secondary structural preferences.

Folding-upon-binding

Nearly one-third of human proteins are intrinsically disordered (IDPs) or contain intrinsically disordered regions (IDRs) that lack a fixed tertiary structure and assume an ensemble of rapidly interconverting conformations. The structural and dynamical plasticity of IDPs expose regions of the polypeptide chain, facilitating post-translational modifications (PTMs) and transient, heterogeneous binding interactions with a diverse range of targets [43]. In some instances, specific ligands, PTMs, or binding interactions can lead to the folding of IDPs [44–46]. NMR spectroscopy is well suited for atomic-level characterizations of such dynamical systems [44]; however, the weak affinities between IDPs and their interaction partners often lead to intermediate exchange

Box 1 NMR methodology to characterize sparsely populated states

At equilibrium, proteins assume a range of interconverting conformational states whose populations are dictated by their relative free energies, with the lowest energy or principally populated conformation referred to as the ground state. Consider two exchanging states, A and B, that interconvert with rate constants k_{AB} and k_{BA} as, $A \underset{k_{BA}}{\overset{k_{AB}}{\rightleftarrows}} B$. The relative populations of the states scale with the Boltzmann distribution, $\frac{p_B}{p_A} = e^{\frac{-\Delta G_{AB}}{RT}}$ and the rates of interconversion depend on the barrier heights that separate the transition state and states A or B, $k_{AB} = \upsilon^{\ddagger} e^{\frac{-\Delta G_{AB}^{\ddagger}}{RT}}$, where R is the universal gas constant, T is the temperature, ΔG_{AB} and $\Delta G_{AB}^{\ddagger}$ are the respective free energy differences between states A and B and between A and the transition state, and $\upsilon^{\ddagger}$ is a pre-exponential factor, which is commonly set to k_BT/h (ca. 6×10^{12} s^{-1}) to match the approximate bond vibration frequency. A more accurate pre-exponential factor [80] would use the transition path time (TPT), or the time required for a successful barrier crossing [81]. TPT values have only recently been measured for small proteins, yielding an average value of ca. 5 μs [81]. Thus, if ΔG_{AB} corresponds to 4RT (2.4 kcal mol^{-1} at 298 K), the percentage of molecules in the minor state will be ~2% of those in the major state. Assuming $\Delta G_{AB}^{\ddagger}$ = 10RT (5.9 kcal mol^{-1}), $\Delta G_{BA}^{\ddagger}$ = 6RT (3.5 kcal mol^{-1} at 298 K) and $\upsilon^{\ddagger}$ is 2×10^5 s^{-1}, obtained from an average TPT of 5 μs, then the interconversion rate $k_{ex} = k_{BA} + k_{AB}$ will be approximately 500 s^{-1}, which is suitable for Carr-Purcell-Meiboom-Gill (CPMG) relaxation dispersion (RD) experiments. When k_{ex} values decrease to approximately 200 s^{-1} or less, the CPMG experiment becomes less sensitive to exchange; in contrast, CEST is better suited for exchange events with k_{ex} values between approximately 20 and 400 s^{-1}.

As might be expected, direct detection of sparsely populated and transiently formed conformers, such as those associated with state B in the preceding example, is exceedingly difficult. Interconversion between two or more conformations on the micro- to millisecond timescale can broaden the detected NMR signals so long as there are differences in chemical shifts or relaxation rates [82] between the interconverting spins.

In favorable cases, RD or CEST can be used to measure multiple NMR parameters of the invisible states, including chemical shifts, residual dipolar couplings [83,84], residual chemical shift anisotropies [85], paramagnetic relaxation enhancements [38], pseudocontact shifts [86], translational diffusion coefficients [87], solvent exchange rates [88,89], and tautomer populations and pK_a values [90]. Dark state exchange saturation transfer (DEST) can be employed to study the kinetics and thermodynamics of exchange between an NMR-visible form and a very large NMR-invisible state, including site-specific transverse relaxation rates of the invisible state [91,92]. New approaches have also been developed that expedite the acquisition of CEST datasets [93–95] and exploit the signal enhancement and other benefits afforded by multiple-quantum spectroscopy [87,96–98].

behavior during NMR titrations, which causes severe broadening and eventual disappearance of cross-peaks for residues directly involved in binding. How, then, can one obtain useful structural and dynamical insight from such systems?

Three recent studies that investigated the folding-upon-binding of IDPs utilized chemical exchange-based NMR methods (Box 1, Figure 2) to measure chemical shifts for the otherwise invisible bound state [47••,48•,49]. The authors prepared samples of the isotopically labeled IDP in the presence of substoichiometric ratios of the binding partner to generate a sparsely populated bound state. The chemical shifts from the invisible bound state could be obtained through chemical exchange NMR methods [44]. By means of example, Ferrage and coworkers used ^{15}N CPMG RD and a combination of CEST experiments (Box 1, Figure 2) from multiple nuclei to determine a structural model of the IDR from the protein Artemis bound to the DNA-binding domain (DBD) of Ligase IV [47••]. By recording CPMG RD and CEST experiments on samples of Artemis in the presence of 0–13% DBD, a complete set of ^{15}N, ^{13}CO, $^{13}C\alpha$, and $^{13}C\beta$ chemical shifts were obtained for DBD-bound Artemis, including residues 485–501 involved in the binding interaction. The NMR data identified additional bound-state dynamics and interactions that were not previously seen in a crystal structure of DBD-bound Artemis fragment 485–495, including an important electrostatic role for Artemis residues 496–501 in modulating the K_d for DBD by a factor of five [47••]. Additional IDP interaction sites were also identified in studies by Delaforge *et al.* [48•] and Milles *et al.* [49], demonstrating the unique ability of NMR spectroscopy to provide atomic-level insight into the binding modes of IDPs [44].

Misfolding

The above examples illustrate how NMR spectroscopy can provide unique mechanistic insight into protein folding by characterizing states that are otherwise invisible to most other biophysical tools. The misfolding of proteins into insoluble amyloid fibrils is implicated in the onset of ca. 40 different human diseases [17]. During the conversion of native proteins into fibrils or other aggregates under physiological conditions, the initial steps of this process generally involve the formation of sparsely populated conformations that are either locally or globally unfolded or that have adopted non-native quaternary structures, such as soluble oligomers or proto-fibrils [50]. Considerable interest has arisen in determining the initial structural changes that eventually culminate in fibril formation or aggregation [51]; however, the atomic-level characterization of these aggregation-prone species remains exceedingly difficult due to their short lifetimes, low populations, and often dynamical conformations. NMR has made significant contributions to our understanding of the structures and dynamics of biomolecular conformations present in the early stages of protein aggregation.

Figure 2

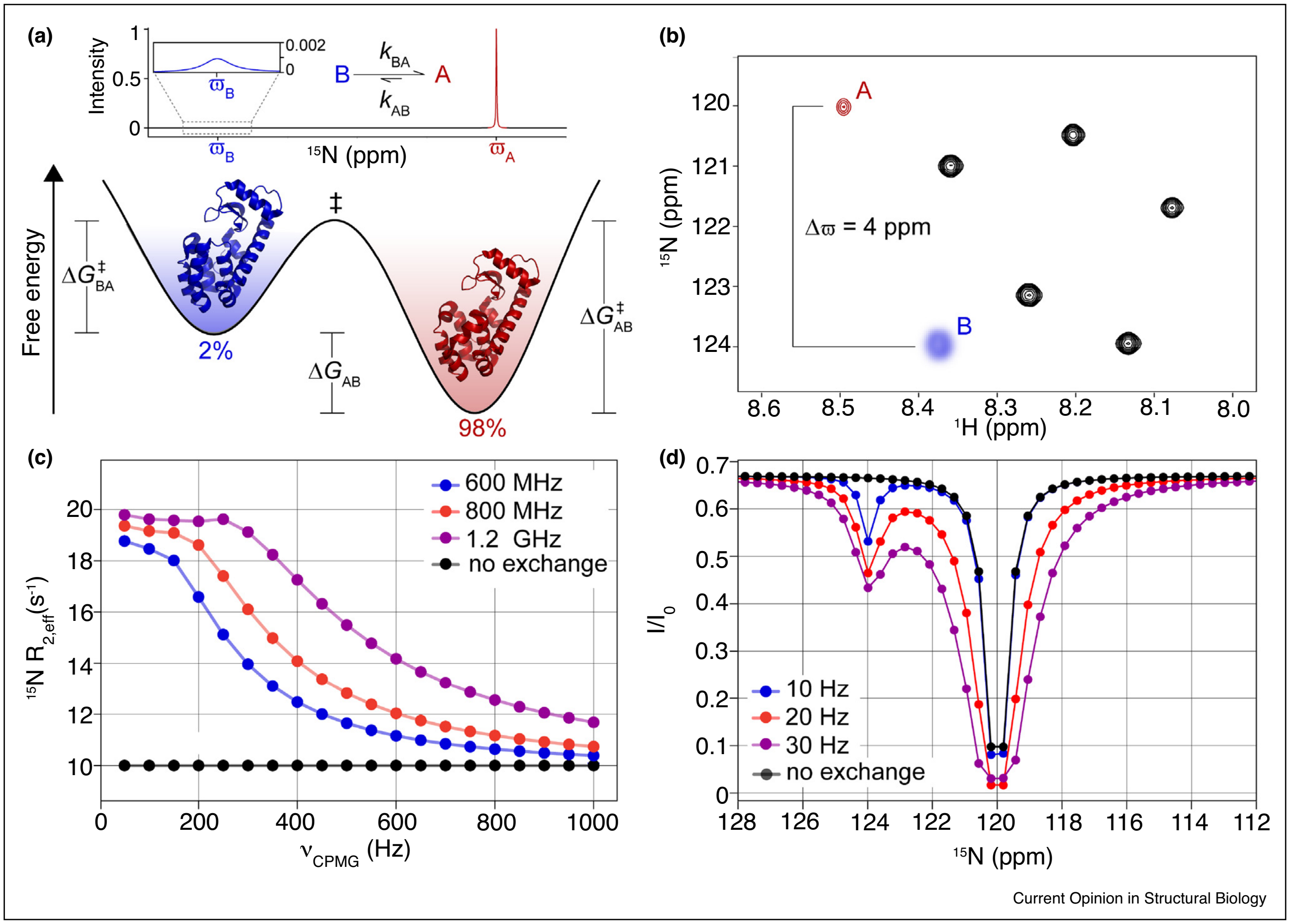

Characterization of sparsely populated or invisible protein states with NMR. **(a)** Bottom: Theoretical free energy landscape depicting two different protein states A (red) and B (blue) separated by a free energy difference ΔG_{AB} = 4RT, corresponding to 2% of state B. The transition state is denoted by the ‡ symbol, and the energy barriers $\Delta G_{AB}^{\ddagger}$ = 10RT and $\Delta G_{BA}^{\ddagger}$ = 6RT separate the respective states from the transition state. Top: Simulated 1D NMR spectrum for a single spin exchanging between two conformations, A and B with p_A (fractional population of the ground, observable state) = 98%, p_B (fractional population of the sparse, invisible state) = 2%, $k_{ex} = k_{AB} + k_{BA}$ = 500 s^{-1}, and $\Delta\varpi$ (difference in chemical shifts between the ground and excited state conformations) = 4 ppm, or 1528 rad s^{-1} at a static magnetic field strength of 14.1 T (corresponding to a ^{1}H resonance frequency of 600 MHz). The intrinsic transverse relaxation rate (R_2) of both states is 10 s^{-1}. The inset shows a zoomed-in region that includes the resonance line derived from state B. In practice, the line would be invisible because of the low population of state B and its transient nature that gives rise to line broadening. **(b)** Example 2D ^{1}H-^{15}N HSQC spectrum highlighting a cross-peak from the observable state A (red) and the corresponding peak from the invisible state B (blue). The cross-peak from state B is blurred because it is not directly observable in the spectrum due to state B's low population and exchange-induced line broadening. **(c)** Chemical exchange NMR methods can provide insight into the kinetics (k_{ex}) and thermodynamics (p_B) of the exchange event, as well as the associated structural changes ($\Delta\varpi$). CPMG RD is ideally suited for systems with k_{ex} values ranging from ca. 200 to 4000 s^{-1}. Shown here are ^{15}N CPMG RD data simulated at three different static magnetic field strengths for the exchanging system shown in panel A. During a fixed relaxation delay, here set to 40 ms, an increasing number of 180° refocusing pulses causes the effective transverse relaxation rate, R_2, to decrease (note that ν_{CPMG} is proportional to the number of 180° pulses). In the absence of exchange, the black data with a flat line are obtained. Note that CPMG RD is sensitive only to the absolute value of $\Delta\varpi$ and thus additional experiments must be performed to delineate the sign, which is crucial for the interpretation of chemical shift changes in context of structural changes. Other chemical exchange approaches such as chemical exchange saturation transfer (CEST) **(d)** provide the sign of the chemical shift difference, but are ideally suited for slower exchange processes, for example, k_{ex} values ranging from ca. 20–400 s^{-1}. Shown here are simulated ^{15}N CEST data at a static magnetic field strength of 14.1 T (corresponding to a ^{1}H resonance frequency of 600 MHz), with an exchange time (T_{EX}) of 400 ms, and a longitudinal relaxation rate of 1 s^{-1} for both states. All other parameters are identical to panels A and C, except that k_{ex} was set to 50 s^{-1}. During T_{EX}, a weak B_1 field of 10 Hz (blue; black, k_{ex} = 0 s^{-1}), 20 Hz (red), or 30 Hz (purple) is swept through the ^{15}N dimension, 'searching' for the peak derived from the excited state. Weak irradiation at the position of the invisible minor state resonance (124 ppm) causes attenuation (I/I_0) of the intensity of the resonance from the observable major state (120 ppm) via chemical exchange.

Local misfolding: β2-microglobulin

Subtle structural rearrangements to the native state of a protein can alter the delicate balance between the folded state and an aggregation-prone conformation, which can have severe physiological consequences. The wild-type form of β2-microglobulin (β2m) undergoes a transition from a structured, soluble protein into toxic amyloid fibrils, which eventually manifest as dialysis-related amyloidosis in individuals who require long-term dialysis due to chronic renal failure [52]. In the native structure of β2m, the protein contains a cis peptidyl-prolyl bond involving residues His31 and Pro32; however, the initiation of amyloid formation proceeds through a transiently formed intermediate where the His31-Pro32 peptide bond has isomerized to a non-native trans conformation (I_T). Interestingly, I_T is also populated during the folding of β2m, indicating that the species responsible for amyloid fibril formation is a native-like protein folding intermediate [52]. A naturally occurring variant of β2m, ΔN6, where the first six residues are proteolytically removed, was found to mimic the conformation of I_T, thereby enabling a detailed NMR investigation of the structure and dynamics of an amyloidogenic intermediate. The non-native trans His31-Pro32 conformer in ΔN6 results in a remodeled hydrophobic core of the protein, leading to the exposure of otherwise buried hydrophobic side-chains and causing an increase in millisecond motions [52]. These millisecond motions were also observed in the I_T conformation present in full-length β2m [53,54], suggesting that conformational fluctuations play a role in the formation of amyloid intermediates [55].

Non-native oligomers: superoxide dismutase 1 and huntingtin

The formation of soluble oligomers often precedes the deposition of insoluble amyloid fibrils or amorphous aggregates. The short lifetimes of such oligomers, however, has rendered them extremely challenging to study at the atomic level, thereby preventing structural insight into pathogenic processes involving self-association. In amyotrophic lateral sclerosis (ALS), superoxide dismutase 1 (SOD1) is deposited into insoluble plaques in motor neurons. Before the appearance of SOD1-containing plaques, however, neurodegeneration can already be detected, which suggests that soluble oligomers of SOD1 may comprise the toxic species. In its mature form, SOD1 exists as a non-covalent dimer (2 × 16 kDa) whose monomers fold into an eight-stranded β-barrel, which each contain one bound ion of Cu, one of Zn, and a single disulfide bond. The holo form of SOD1 is ultra-stable, with a melting temperature over 90°C; in contrast, the apo, reduced form of the protein (apoSOD1^{2SH}) melts near 45°C and misfolds and aggregates *in vitro*. Therefore, apoSOD1^{2SH} is a likely candidate for the species responsible for the pathogenic aggregation of SOD1.

A series of NMR papers performed both inside living cells and *in vitro* unraveled the structural and dynamical events that accompany the maturation of SOD1 [56–61]. Fluctuations in two loop regions of apoSOD1^{2SH} cause the transient formation of at least four sparsely populated states with populations ranging from 2 to 3% and lifetimes of 2–13 ms [56]. These conformers, which were not detected in the mature version of SOD1 [57], were otherwise invisible in the NMR spectra of apoSOD1^{2SH} and could only be structurally characterized through the combination of CPMG and CEST experiments (Box 1, Figure 2). Two of the minor states of apoSOD1^{2SH} adopt structural elements that resemble conformations found in mature SOD1, suggesting a transient sampling of the maturation pathway, whereas the other two states form non-native oligomers [56]. These separate misfolding pathways in apoSOD1^{2SH} likely contribute to its destabilization *in vitro*, which is significantly enhanced by crowding agents that cause it to unfold at much lower temperatures [58]. Similar observations have been reported inside the crowded environment of mammalian cells, where NMR spectra of apoSOD1^{2SH} revealed a significantly unfolded form before the binding of metals [59,60].

These studies offered insight into the maturation pathway of WT SOD1 and pinpointed structural and dynamical transitions in the immature protein that perhaps contribute to its pathogenic aggregation in ALS. Mutations in SOD1 account for nearly 20% of the familial cases of ALS (fALS). Seven different ALS-causing mutations in SOD1 were recently studied in order to characterize their free energy landscapes and thermally accessible conformers [61]. Interestingly, while the mutations lowered the ΔG of unfolding and thereby destabilized the folded state, the ground state structures and dynamics of all studied mutants were highly similar to the WT protein, suggesting that alterations to the native structure were not responsible for aggregation. Instead, the mutants displayed significantly altered populations and lifetimes of the minor states that had been observed previously in the WT protein [61]. Moreover, new minor states involving structural transitions in the β5/β6 cleft were observed for the G85R and G93A ALS-causing variants of SOD1, pointing to a dynamic hotspot that might play a role in SOD1 aggregation [61].

The protein huntingtin aggregates into fibrils and causes the neurodegenerative disorder referred to as Huntington's disease. Kotler *et al.* utilized a combination of NMR and EPR spectroscopy to investigate the initial steps involved in the formation of huntingtin fibrils [62••]. Using a truncated version of huntingtin that contains the N-terminal region and seven glutamine residues (htt^{NT}Q$_7$), the authors collected NMR experiments sensitive to conformational exchange over a range of protein concentrations. While the htt^{NT}Q$_7$ monomer populates a predominantly disordered conformation, a transiently populated species was detected whose backbone ^{15}N and $^{13}C\alpha$ chemical shifts contained significant helical character. Modelling of the minor state using intermolecular paramagnetic relaxation enhancement (PRE) measurements and the measured chemical shifts revealed the formation of a helical dimer and tetramer, which were validated through DEER and CW EPR data [62••]. The binding of htt^{NT}Q$_{10}$, which contained an additional three glutamine residues, to lipid vesicles was investigated with ^{15}N, $^{13}C\alpha$, $^{13}C\beta$, and ^{13}CO CEST experiments, which revealed the formation of a 15-residue helix [63]. EPR data indicated that the partially helical bound form of htt^{NT}Q$_{10}$ can dimerize on the vesicle surface, thus providing mechanistic insight into lipid-catalyzed aggregation [63].

Dissociation of native oligomers: transthyretin and immunoglobulin light chain

Whereas non-native oligomers can contribute to the onset of pathogenic protein misfolding diseases, a significant number of proteins natively form soluble oligomers and bury large hydrophobic surface areas [64]. For instance, between 35–45% of the 689 protein-coding genes in the organism Mycoplasma pneumoniae, which has one of the smallest genomes, were found to encode proteins that oligomerize [65]. In the human proteome, destabilization of native oligomers, either through inherent quaternary dynamics or destabilizing mutations, can expose hydrophobic regions to the cellular milieu and can contribute to protein aggregation (Figure 1). In an amyloidosis caused by the dissociation of a native tetramer, the stabilization of its quaternary contacts with a small molecule was found to slow down disease progression [66]. Thus, a clear need arises for understanding the conformational dynamics of amyloidogenic oligomers.

Transthyretin (TTR) exists in its native state as a structured tetramer, but the protein readily forms amyloid fibrils with over 100 autosomal dominant mutations that have been identified in amyloid-related disorders. Before amyloid formation, however, the TTR tetramer must first dissociate into monomers that remain structured but have widespread millisecond motions [69]. In addition, the TTR tetramer itself has interesting dynamics: ^{19}F NMR studies identified a small population (7%) of wild-type TTR tetramers with a mispacked F87 sidechain, which were severely destabilized and prone to aggregation [70]. Moreover, relaxation dispersion studies on pathogenic variants of TTR showed that they also sample thermally accessible excited states with perturbed subunit interfaces, providing a structural rationale for why tetramers of the disease-implicated variants are more destabilized [71]. The aggregation kinetics of these TTR variants were studied in real-time with ^{19}F NMR, identifying various species populated along the aggregation pathway [72].

Among systemic amyloid diseases, the most commonly diagnosed form involves the aggregation and fibril formation of different immunoglobulin (Ig) antibody light chains (LCs) within Ig LC amyloidosis patients. Full-length Ig LC proteins exist as dimers of monomers comprised of an N-terminal variable domain (V_L) and a C-terminal constant domain (C_L), with inter-protomer V_L–V_L, C_L–C_L, and intra-protomer V_L–C_L interactions burying a combined surface area of approximately 4500 Å^2. Previous work established that monomeric forms of Ig LCs and their constituent isolated domains are aggregation-prone and readily form fibrils [67]. To assess the relative contributions to aggregation from the isolated domains and monomers or dimers, Rennella *et al.* [68] studied two LC variants that have identical C_L domains but only 84% sequence identity in their V_L domains, termed the JTO and WIL variants. Interestingly, CPMG RD and chemical shift changes revealed that the dimerization K_d values for the individual JTO and WIL V_L domains differed by nearly three orders of magnitude (ca. 10 μM vs ~5 mM), and that the isolated C_L domain only weakly associated with a dimerization K_d (ca. 10 mM) similar to the WIL V_L dimer. In context of the full-length proteins, however, the situation is much different: for both the JTO and WIL variants, the V_L–V_L dimer interface was 100% populated and the C_L–C_L dimer interface was populated to over 90%. Thus, positive cooperativity exists between the domains that promotes favorable interactions in the full-length protein. The unique ability of NMR spectroscopy to probe the contributions from individual domains in the full-length protein, in combination with functional assays, revealed that the C_L domain is protective against aggregation. A monomeric LC with an intact C_L domain was recalcitrant to aggregation, whereas LC dimers with destabilized C_L domains were highly susceptible to aggregation.

Perspectives and outlook

Proteins frequently make transient excursions to thermally accessible, higher energy conformations with lifetimes on the order of a few milliseconds. While the low populations of such states render them effectively 'invisible' to most biophysical methods, including some NMR experiments, chemical exchange-based and other NMR methods can characterize the structures and dynamics of these states at the atomic level. Such studies have provided rich biological insight, including descriptions of on-pathway folding intermediates, aggregation-prone misfolded states, and soluble oligomers that precede amyloid fibril formation. NMR-derived descriptions of invisible protein states have injected fresh insight into model systems: for example, an invisible state in the protein ubiquitin was found to expose a phosphosite and act as a better substrate for the kinase PINK1 [73]. In addition to solution-state NMR, advancements in the field of solid-state NMR have enabled detailed studies of invisible, excited states [74]. In closing, we emphasize the importance of the development of NMR methodology (Box 1) in driving the field forward [15], with significant contributions from new hardware [75], software [76], isotope labeling strategies [77], and pulse sequences [78]. Presently unforeseen biological insight will indubitably be obtained from future studies that make use of yet unrealized NMR methodology [79].

Conflict of interest statement

Nothing declared.

Acknowledgements

This work was supported by grants from the Canadian Institutes of Health Research and the Natural Sciences and Engineering Research Council of Canada (to L.E.K.) and a Banting Postdoctoral Fellowship (to T.R.A). L.E. K. holds a Canada Research Chair in Biochemistry.

References and recommended reading

Papers of particular interest, published within the period of review, have been highlighted as:

- • of special interest
- •• of outstanding interest

1. Henzler-Wildman K, Kern D: **Dynamic personalities of proteins**. *Nature* 2007, **450**:964-972.

2. Baldwin AJ, Kay LE: **NMR spectroscopy brings invisible protein states into focus**. *Nat Chem Biol* 2009, **5**:808-814.

3. Wright PE, Dyson HJ: **Intrinsically disordered proteins in cellular signalling and regulation**. *Nat Rev Mol Cell Biol* 2015, **16**:18-29.

4. Smock RG, Gierasch LM: **Sending signals dynamically**. *Science* 2009, **324**:198-203.

5. Motlagh HN, Wrabl JO, Li J, Hilser VJ: **The ensemble nature of allostery**. *Nature* 2014, **508**:331-339.

6. •• Sekhar A, Kay LE: **An NMR view of protein dynamics in health and disease**. *Annu Rev Biophys* 2019, **48** annurev-biophys-052118-115647

Informative review on NMR-derived insight into dysregulated protein dynamics in human diseases.

7. Stein A, Fowler DM, Hartmann-Petersen R, Lindorff-Larsen K: **Biophysical and mechanistic models for disease-causing protein variants**. *Trends Biochem Sci* 2019, **44**:575-588.

8. Schuetz AK, Kay LE: **A Dynamic molecular basis for malfunction in disease mutants of p97/VCP**. *eLife* 2016, **5**.

9. Toyama Y, Kano H, Mase Y, Yokogawa M, Osawa M, Shimada I: **Dynamic regulation of GDP binding to G proteins revealed by magnetic field-dependent NMR relaxation analyses**. *Nat Commun* 2017, **8**:14523.

10. Toyama Y, Kontani K, Katada T, Shimada I: **Conformational landscape alternations promote oncogenic activities of Ras-related C3 botulinum toxin substrate 1 as revealed by NMR**. *Sci Adv* 2019, **5**:eaav8945.

11. Saleh T, Rossi P, Kalodimos CG: **Atomic view of the energy landscape in the allosteric regulation of Abl kinase**. *Nat Struct Mol Biol* 2017, **24**:893-901.

12. •• Kimsey IJ, Szymanski ES, Zahurancik WJ, Shakya A, Xue Y, Chu C-C, Sathyamoorthy B, Suo Z, Al-Hashimi HM: **Dynamic basis for dG•dT misincorporation via tautomerization and ionization**. *Nature* 2018, **554**:195-201

Direct NMR evidence for the presence of sparsely populated dG•dT tautomers. Computational modeling based on the NMR data indicates that DNA polymerases misincorporate dG•dT base pairs because of this sparsely populated state.

13. Boehr DD, Nussinov R, Wright PE: **The role of dynamic conformational ensembles in biomolecular recognition**. *Nat Chem Biol* 2009, **5**:789-796.

14. Mittermaier AK, Kay LE: **Observing biological dynamics at atomic resolution using NMR**. *Trends Biochem Sci* 2009, **34**:601-611.

15. Arthanari H, Takeuchi K, Dubey A, Wagner G, Voth G, Yeager M: **Emerging solution NMR methods to illuminate the structural and dynamic properties of proteins**. *Curr Opin Struct Biol* 2019, **52** S0959-440X(18)30113-1.

16. • Zhuravleva A, Korzhnev DM: **Protein folding by NMR**. *Prog Nucl Magn Reson Spectrosc* 2017, **100**:52-77

Comprehensive review on protein folding studied by NMR, which outlines chemical exchange approaches such as CPMG and $R_{1\rho}$ relaxation dispersion, CEST, PREs, and ZZ exchange, among others.

17. Chiti F, Dobson CM: **Protein misfolding, amyloid formation, and human disease: a summary of progress over the last decade**. *Annu Rev Biochem* 2017, **86**:27-68.

18. Roche J, Royer CA, Roumestand C: **Exploring protein conformational landscapes using high-pressure NMR**. *Methods Enzymol* 2019:293-320.

19. Tugarinov V, Libich DS, Meyer V, Roche J, Clore GM: **The energetics of a three-state protein folding system probed by high-pressure relaxation dispersion NMR spectroscopy**. *Angew Chem Int Ed* 2015, **54**:11157-11161.

20. Zhang Y, Kitazawa S, Peran I, Stenzoski N, McCallum SA, Raleigh DP, Royer CA: **High pressure ZZ-exchange NMR reveals key features of protein folding transition states**. *J Am Chem Soc* 2016, **138**:15260-15266.

21. Alderson TR, Charlier C, Torchia DA, Anfinrud P, Bax A: **Monitoring hydrogen exchange during protein folding by fast pressure jump NMR spectroscopy**. *J Am Chem Soc* 2017, **139**:11036-11039.

22. •• Charlier C, Alderson TR, Courtney JM, Ying J, Anfinrud P, Bax A: **Study of protein folding under native conditions by rapidly switching the hydrostatic pressure inside an NMR sample cell**. *Proc Natl Acad Sci U S A* 2018, **115**:E4169-E4178

Outlines novel pressure-jump hardware to rapidly change the pressure inside a commercially available NMR sample cell. Demonstration of parallel folding pathways with an on-pathway folding intermediate.

23. Charlier C, Courtney JM, Alderson TR, Anfinrud P, Bax A: **Monitoring ^{15}N chemical shifts during protein folding by pressure-jump NMR**. *J Am Chem Soc* 2018, **140**:8096-8099.

24. Charlier C, Courtney JM, Anfinrud P, Bax A: **Interrupted pressure-jump NMR experiments reveal resonances of on-pathway protein folding intermediate**. *J Phys Chem B* 2018, **122**:11792-11799.

25. Pustovalova Y, Kukic P, Vendruscolo M, Korzhnev DM: **Probing the residual structure of the low populated denatured state of ADA2h under folding conditions by relaxation dispersion nuclear magnetic resonance spectroscopy**. *Biochemistry* 2015, **54**:4611-4622.

26. Kukic P, Pustovalova Y, Camilloni C, Gianni S, Korzhnev DM, Vendruscolo M: **Structural characterization of the early events in the nucleation–condensation mechanism in a protein folding process**. *J Am Chem Soc* 2017, **139**:6899-6910.

27. Sanchez-Medina C, Sekhar A, Vallurupalli P, Cerminara M, Muñoz V, Kay LE: **Probing the free energy landscape of the fast-folding gpW protein by relaxation dispersion NMR**. *J Am Chem Soc* 2014, **136**:7444-7451.

28. Reddy JG, Pratihar S, Ban D, Frischkorn S, Becker S, Griesinger C, Lee D: **Simultaneous determination of fast and slow dynamics in molecules using extreme CPMG relaxation dispersion experiments**. *J Biomol NMR* 2018, **70**:1-9.

29. Vahidi S, Ripstein ZA, Bonomi M, Yuwen T, Mabanglo MF, Juravsky JB, Rizzolo K, Velyvis A, Houry WA, Vendruscolo M *et al.*: **Reversible inhibition of the ClpP protease via an N-terminal conformational switch**. *Proc Natl Acad Sci U S A* 2018, **115**:E6447-E6456.

30. Hiller S, Burmann BM: **Chaperone–client complexes: a dynamic liaison**. *J Magn Reson* 2018, **289**:142-155.

31. Alderson TR, Roche J, Gastall HY, Dias DM, Pritišanac I, Ying J, Bax A, Benesch JLP, Baldwin AJ: **Local unfolding of the HSP27 monomer regulates chaperone activity**. *Nat Commun* 2019, **10**:1068.

32. • Weinhäupl K, Lindau C, Hessel A, Wang Y, Schütze C, Jores T, Melchionda L, Schönfisch B, Kalbacher H, Bersch B *et al.*: **Structural basis of membrane protein chaperoning through the mitochondrial intermembrane space**. *Cell* 2018, **175**:1365-1379.e25

NMR study making use of specific methyl-labeling approaches to investigate the dynamics of a large, molecular chaperone complex that interacts with membrane proteins. The NMR data are used to guide subsequent cell biology experiments.

33. Hiller S: **Chaperone-bound clients: the importance of being dynamic**. *Trends Biochem Sci* 2019, **44**:517-527.

34. Deshmukh L, Tugarinov V, Louis JM, Clore GM: **Binding kinetics and substrate selectivity in HIV-1 protease−Gag interactions probed at atomic resolution by chemical exchange NMR**. *Proc Natl Acad Sci U S A* 2017, **114**:E9855-E9862.

35. Libich DS, Tugarinov V, Ghirlando R, Clore GM: **Confinement and stabilization of Fyn SH3 folding intermediate mimetics within the cavity of the chaperonin GroEL demonstrated by relaxation-based NMR**. *Biochemistry* 2017, **56**:903-906.

36. Huang R, Ripstein ZA, Augustyniak R, Lazniewski M, Ginalski K, Kay LE, Rubinstein JL: **Unfolding the mechanism of the AAA+ unfoldase VAT by a combined cryo-EM, solution NMR study**. *Proc Natl Acad Sci U S A* 2016, **113**:E4190-E4199.

37. Augustyniak R, Kay LE: **Cotranslocational processing of the protein substrate calmodulin by an AAA+ unfoldase occurs via unfolding and refolding intermediates**. *Proc Natl Acad Sci U S A* 2018, **115**:E4786-E4795.

38. Sekhar A, Rosenzweig R, Bouvignies G, Kay LE: **Hsp70 biases the folding pathways of client proteins**. *Proc Natl Acad Sci U S A* 2016, **113**:E2794-E2801.

39. Sekhar A, Rosenzweig R, Bouvignies G, Kay LE: **Mapping the conformation of a client protein through the Hsp70 functional cycle**. *Proc Natl Acad Sci U S A* 2015, **112**:10395-10400.

40. • Sekhar A, Velyvis A, Zoltsman G, Rosenzweig R, Bouvignies G, Kay LE: **Conserved conformational selection mechanism of Hsp70 chaperone-substrate interactions**. *eLife* 2018, **7**

Direct evidence for Hsp70 molecular chaperones using a conformational selection mechanism, whereby the transiently unfolded form of a substrate protein is specifically selected from the ensemble of conformers. NMR chemical exchange experiments that quantify rate constants and subsequent data modeling provided unambiguous results.

41. Vallurupalli P, Sekhar A, Yuwen T, Kay LE: **Probing conformational dynamics in biomolecules via chemical exchange saturation transfer: a primer**. *J Biomol NMR* 2017, **67**:243-271.

42. Farrow NA, Zhang O, Forman-Kay JD, Kay LE: **A heteronuclear correlation experiment for simultaneous determination of 15N longitudinal decay and chemical exchange rates of systems in slow equilibrium**. *J Biomol NMR* 1994, **4**:727-734.

43. Pritišanac I, Vernon RM, Moses AM, Forman-Kay JD: **Entropy and information within intrinsically disordered protein regions**. *Entropy* 2019, **21**:662.

44. Schneider R, Blackledge M, Jensen MR: **Elucidating binding mechanisms and dynamics of intrinsically disordered protein complexes using NMR spectroscopy**. *Curr Opin Struct Biol* 2019, **54**:10-18.

45. Bah A, Vernon RM, Siddiqui Z, Krzeminski M, Muhandiram R, Zhao C, Sonenberg N, Kay LE, Forman-Kay JD: **Folding of an intrinsically disordered protein by phosphorylation as a regulatory switch**. *Nature* 2015, **519**:106-109.

46. Ocasio VJ, Corrêa F, Gardner KH: **Ligand-induced folding of a two-component signaling receiver domain**. *Biochemistry* 2015, **54**:1353-1363.

47. •• Charlier C, Bouvignies G, Pelupessy P, Walrant A, Marquant R, Kozlov M, De Ioannes P, Bolik-Coulon N, Sagan S, Cortes P *et al.*: **Structure and dynamics of an intrinsically disordered protein region that partially folds upon binding by chemical-exchange NMR**. *J Am Chem Soc* 2017, **139**:12219-12227

NMR-driven structural model of a disordered protein bound to its folded partner. The model relied on chemical shifts for the invisible bound state that were obtained with CPMG relaxation dispersion and CEST. An important role is identified for regions beyond those observed in an earlier crystal structure.

48. • Delaforge E, Kragelj J, Tengo L, Palencia A, Milles S, Bouvignies G, Salvi N, Blackledge M, Jensen MR: **Deciphering the dynamic interaction profile of an intrinsically disordered protein by NMR exchange spectroscopy**. *J Am Chem Soc* 2018, **140**:1148-1158

Structural description of an IDP binding to its folded partner, making use of CPMG relaxation dispersion and CEST to provide chemical shifts and transverse relaxation rates for the bound state. The transverse relaxation rates of the bound IDP are extracted from the data and reveal multiple dynamical binding modes.

49. Milles S, Jensen MR, Lazert C, Guseva S, Ivashchenko S, Communie G, Maurin D, Gerlier D, Ruigrok RWH, Blackledge M: **An ultraweak interaction in the intrinsically disordered replication machinery is essential for measles virus function**. *Sci Adv* 2018, **4**:eaat7778.

50. Neudecker P, Robustelli P, Cavalli A, Walsh P, Lundstrom P, Zarrine-Afsar A, Sharpe S, Vendruscolo M, Kay LE: **Structure of an intermediate state in protein folding and aggregation**. *Science* 2012, **336**:362-366.

51. Karamanos TK, Kalverda AP, Thompson GS, Radford SE: **Mechanisms of amyloid formation revealed by solution NMR**. *Prog Nucl Magn Reson Spectrosc* 2015, **88–89**:86-104.

52. Eichner T, Radford SE: **Understanding the complex mechanisms of β2-microglobulin amyloid assembly**. *FEBS J* 2011, **278**:3868-3883.

53. Rennella E, Cutuil T, Schanda P, Ayala I, Forge V, Brutscher B: **Real-time NMR characterization of structure and dynamics in a transiently populated protein folding intermediate**. *J Am Chem Soc* 2012, **134**:8066-8069.

54. Rennella E, Cutuil T, Schanda P, Ayala I, Gabel F, Forge V, Corazza A, Esposito G, Brutscher B: **Oligomeric states along the folding pathways of β2-microglobulin: kinetics, thermodynamics, and structure**. *J Mol Biol* 2013, **425**:2722-2736.

55. Karamanos TK, Pashley CL, Kalverda AP, Thompson GS, Mayzel M, Orekhov VY, Radford SE: **A population shift between sparsely populated folding intermediates determines amyloidogenicity**. *J Am Chem Soc* 2016, **138**:6271-6280.

56. Sekhar A, Rumfeldt JA, Broom HR, Doyle CM, Bouvignies G, Meiering EM, Kay LE: **Thermal fluctuations of immature SOD1 lead to separate folding and misfolding pathways**. *eLife* 2015, **4**:e07296.

57. Culik RM, Sekhar A, Nagesh J, Deol H, Rumfeldt JAO, Meiering EM, Kay LE: **Effects of maturation on the conformational free-energy landscape of SOD1**. *Proc Natl Acad Sci U S A* 2018, **115**:E2546-E2555.

58. Bille A, Jensen KS, Mohanty S, Akke M, Irbäck A: **Stability and local unfolding of SOD1 in the presence of protein crowders**. *J Phys Chem B* 2019, **123**:1920-1930.

59. Banci L, Barbieri L, Bertini I, Luchinat E, Secci E, Zhao Y, Aricescu AR: **Atomic-resolution monitoring of protein maturation in live human cells by NMR**. *Nat Chem Biol* 2013, **9**:297-299.

60. Luchinat E, Barbieri L, Rubino JT, Kozyreva T, Cantini F, Banci L: **In-cell NMR reveals potential precursor of toxic species from SOD1 fALS mutants**. *Nat Commun* 2014, **5**:5502.

61. Sekhar A, Rumfeldt JAO, Broom HR, Doyle CM, Sobering RE, Meiering EM, Kay LE: **Probing the free energy landscapes of ALS disease mutants of SOD1 by NMR spectroscopy**. *Proc Natl Acad Sci U S A* 2016, **113**:E6939-E6945.

62. Kotler SA, Tugarinov V, Schmidt T, Ceccon A, Libich DS,
•• Ghirlando R, Schwieters CD, Clore GM: **Probing initial transient oligomerization events facilitating Huntingtin fibril nucleation at atomic resolution by relaxation-based NMR**. *Proc Natl Acad Sci U S A* 2019, **116**:3562-3571

Insight into the early events associated with the aggregation of the N-terminal region of Huntingtin. Kinetic modeling based on NMR data — namely, exchange-induced shifts and CPMG relaxation dispersion recorded for multiple nuclei — obtained across a wide range of concentrations provides insight into the early steps involved in aggregation. Structural modeling based on chemical shifts derived from CPMG relaxation dispersion and CEST, combined with longer-range distance restraints derived from inter-molecular PREs, lead to a model of the sparsely populated tetramer. EPR data are used as an independent validation.

63. Ceccon A, Schmidt T, Tugarinov V, Kotler SA, Schwieters CD, Clore GM: **Interaction of huntingtin exon-1 peptides with lipid-based micellar nanoparticles probed by solution NMR and Q-band pulsed EPR**. *J Am Chem Soc* 2018, **140**:6199-6202.

64. Marsh JA, Teichmann SA: **Structure, dynamics, assembly, and evolution of protein complexes**. *Annu Rev Biochem* 2015, **84**:551-575.

65. Kühner S, van Noort V, Betts MJ, Leo-Macias A, Batisse C, Rode M, Yamada T, Maier T, Bader S, Beltran-Alvarez P *et al.*: **Proteome organization in a genome-reduced bacterium**. *Science* 2009, **326**:1235-1240.

66. Johnson SM, Connelly S, Fearns C, Powers ET, Kelly JW: **The Transthyretin amyloidoses: from delineating the molecular mechanism of aggregation linked to pathology to a regulatory-agency-approved drug**. *J Mol Biol* 2012, **421**:185-203.

67. Brumshtein B, Esswein SR, Landau M, Ryan CM, Whitelegge JP, Phillips ML, Cascio D, Sawaya MR, Eisenberg DS: **Formation of amyloid fibers by monomeric light chain variable domains**. *J Biol Chem* 2014, **289**:27513-27525.

68. Rennella E, Morgan GJ, Kelly JW, Kay LE: **Role of domain interactions in the aggregation of full-length immunoglobulin light chains**. *Proc Natl Acad Sci U S A* 2019, **116**:854-863.

69. Lim KH, Dyson HJ, Kelly JW, Wright PE: **Localized structural fluctuations promote amyloidogenic conformations in transthyretin**. *J Mol Biol* 2013, **425**:977-988.

70. Sun X, Jaeger M, Kelly JW, Dyson HJ, Wright PE: **Mispacking of the Phe87 Side Chain Reduces the Kinetic Stability of Human Transthyretin**. *Biochemistry* 2018, **57**:6919-6922.

71. Leach BI, Zhang X, Kelly JW, Dyson HJ, Wright PE: **NMR measurements reveal the structural basis of transthyretin destabilization by pathogenic mutations**. *Biochemistry* 2018, **57**:4421-4430.

72. Sun X, Dyson HJ, Wright PE: **Kinetic analysis of the multistep aggregation pathway of human transthyretin**. *Proc Natl Acad Sci U S A* 2018, **115**:E6201-E6208.

73. Gladkova C, Schubert AF, Wagstaff JL, Pruneda JN, Freund SM, Komander D: **An invisible ubiquitin conformation is required for efficient phosphorylation by PINK1**. *EMBO J* 2017, **36**:3555-3572.

74. Gauto DF, Macek P, Barducci A, Fraga H, Hessel A, Terauchi T, Gajan D, Miyanoiri Y, Boisbouvier J, Lichtenecker R *et al.*: **Aromatic ring dynamics, thermal activation, and transient conformations of a 468 kDa enzyme by specific 1H– 13C labeling and fast magic-angle spinning NMR**. *J Am Chem Soc* 2019, **141**:11183-11195.

75. Kupče Ē, Mote KR, Madhu PK: **Experiments with direct detection of multiple FIDs**. *J Magn Reson* 2019, **304**:16-34.

76. Pritišanac I, Degiacomi MT, Alderson TR, Carneiro MG, Ab E, Siegal G, Baldwin AJ: **Automatic assignment of methyl-NMR spectra of supramolecular machines using graph theory**. *J Am Chem Soc* 2017, **139**:9523-9533.

77. Boeszoermenyi A, Chhabra S, Dubey A, Radeva DL, Burdzhiev NT, Chanev CD, Petrov OI, Gelev VM, Zhang M, Anklin C *et al.*: **Aromatic ^{19}F-^{13}C TROSY: a background-free approach to probe biomolecular structure, function, and dynamics**. *Nat Methods* 2019, **16**:333-340.

78. Pritchard RB, Hansen DF: **Characterising side chains in large proteins by protonless 13C-detected NMR spectroscopy**. *Nat Commun* 2019, **10**:1747.

79. Bax A, Clore GM: **Protein NMR: boundless opportunities**. *J Magn Reson* 2019, **306**:187-191.

80. Vallurupalli P, Chakrabarti N, Pomès R, Kay LE: **Atomistic picture of conformational exchange in a T4 lysozyme cavity mutant: an experiment-guided molecular dynamics study**. *Chem Sci* 2016, **7**:3602-3613.

81. Chung HS, Eaton WA: **Protein folding transition path times from single molecule FRET**. *Curr Opin Struct Biol* 2018, **48**:30-39.

82. Yuwen T, Brady JP, Kay LE: **Probing conformational exchange in weakly interacting, slowly exchanging protein systems via off-resonance R $_{1\rho}$ experiments: application to studies of protein phase separation**. *J Am Chem Soc* 2018, **140**:2115-2126.

83. Zhao B, Zhang Q: **Measuring residual dipolar couplings in excited conformational states of nucleic acids by CEST NMR spectroscopy**. *J Am Chem Soc* 2015, **137**:13480-13483.

84. Vallurupalli P, Hansen DF, Stollar E, Meirovitch E, Kay LE: **Measurement of bond vector orientations in invisible excited states of proteins**. *Proc Natl Acad Sci U S A* 2007, **104**:18473-18477.

85. Vallurupalli P, Hansen DF, Kay LE: **Probing structure in invisible protein states with anisotropic NMR chemical shifts**. *J Am Chem Soc* 2008, **130**:2734-2735.

86. Ma RS, Li QF, Wang AD, Zhang JH, Liu ZJ, Wu JH, Su XC, Ruan K: **Determination of pseudocontact shifts of low-populated excited states by NMR chemical exchange saturation transfer**. *Phys Chem Chem Phys* 2016, **18**:13794-13798.

87. Yuwen T, Sekhar A, Baldwin AJ, Vallurupalli P, Kay LE: **Measuring diffusion constants of invisible protein conformers by triple-quantum 1H CPMG relaxation dispersion**. *Angew Chemie Int Ed* 2018, **57**:16777-16780.

88. Long D, Bouvignies G, Kay LE: **Measuring hydrogen exchange rates in invisible protein excited states**. *Proc Natl Acad Sci U S A* 2014, **111**:8820-8825.

89. Yuwen T, Bah A, Brady JP, Ferrage F, Bouvignies G, Kay LE: **Measuring solvent hydrogen exchange rates by multifrequency excitation ^{15}N CEST: application to protein phase separation**. *J Phys Chem B* 2018, **122**:11206-11217.

90. Hansen AL, Kay LE: **Measurement of histidine pK_a values and tautomer populations in invisible protein states**. *Proc Natl Acad Sci U S A* 2014, **111**:E1705-E1712.

91. Ceccon A, Tugarinov V, Bax A, Clore GM: **Global dynamics and exchange kinetics of a protein on the surface of nanoparticles revealed by relaxation-based solution NMR spectroscopy**. *J Am Chem Soc* 2016, **138**:5789-5792.

92. Ceccon A, Clore GM, Tugarinov V: **Decorrelating kinetic and relaxation parameters in exchange saturation transfer NMR: a case study of n-terminal huntingtin peptides binding to unilamellar lipid vesicles**. *J Phys Chem B* 2018, **122**:11271-11278.

93. Yuwen T, Kay LE, Bouvignies G: **Dramatic decrease in cest measurement times using multi-site excitation**. *ChemPhysChem* 2018, **19**:1707-1710.

94. Yuwen T, Bouvignies G, Kay LE: **Exploring methods to expedite the recording of CEST datasets using selective pulse excitation**. *J Magn Reson* 2018, **292**:1-7.

95. Leninger M, Marsiglia WM, Jerschow A, Traaseth NJ: **Multiple frequency saturation pulses reduce CEST acquisition time for quantifying conformational exchange in biomolecules**. *J Biomol NMR* 2018, **71**:19-30.

96. Yuwen T, Vallurupalli P, Kay LE: **Enhancing the sensitivity of CPMG relaxation dispersion to conformational exchange**

processes by multiple-quantum spectroscopy. *Angew Chemie Int Ed* 2016, **55**:11490-11494.

97. Toyama Y, Osawa M, Yokogawa M, Shimada I: **NMR method for characterizing microsecond-to-millisecond chemical exchanges utilizing differential multiple-quantum relaxation in high molecular weight proteins**. *J Am Chem Soc* 2016, **138**:2302-2311.

98. Gopalan AB, Yuwen T, Kay LE, Vallurupalli P: **A methyl 1H double quantum CPMG experiment to study protein conformational exchange**. *J Biomol NMR* 2018, **72**:79-91.